

# Influence of a Novel Superabsorbent Slow-release Fertilizer and Water Deficit on Herbage Biomass and oil Production of *Thymus daenensis*

Jahangir Abedi-Koupai<sup>1</sup>, Mina Baki<sup>2</sup>, and Mohammad Javad Amiri<sup>3\*</sup>

<sup>1</sup>Professor, Department of Water Science and Engineering, College of Agriculture, Isfahan University of Technology, Isfahan, 84156-83111, Iran

<sup>2</sup>Former Ph.D. Student, Department of Water Science and Engineering, College of Agriculture, Isfahan University of Technology, Isfahan, 84156-83111, Iran

<sup>3</sup>Associate Professor, Department of Water Engineering, Faculty of Agriculture, Fasa University, Fasa 74616-86131, Iran

\*Corresponding author: Email: mj\_amiri@fasau.ac.ir

Article History: Received: 30 November 2023/Accepted in revised form: 06 January 2024

© 2012 Iranian Society of Medicinal Plants. All rights reserved

## ABSTRACT

Fertilizers and water play critical roles in supporting plant growth, and enhancing the efficiency of their application is essential, especially in drought-affected regions, to maximize the utilization of these vital resources. In this study, our objective was to examine the impact of water deficit stress and a superabsorbent slow-release fertilizer (SSRF) on the growth, yield, and oil production of *Thymus daenensis*. The experiments were conducted using a total of 27 drainage lysimeters to ensure accurate measurements and observations. The experiment was designed as a completely randomized factorial design, specifically investigating the effects of three fertilizer rates (0, 10, and 50 Mg ha<sup>-1</sup>) and three irrigation regimes (50%, 70%, and 100% of water requirement). The synthesis of the SSRF involved the graft-copolymerization of acrylic acid and acrylamide onto sodium alginate and rapeseed meal biochar. The preparation of the biochar was carried out at a temperature of 300 °C. The surface morphology analysis of the SSRF provided evidence for the successful occurrence of graft polymerization. Additionally, the graft copolymers exhibited a significant nitrogen content, which greatly contributed to their high free-absorbency capacity of 40%. as determined by the tea bag method. The results of the study indicate that water stress had a negative impact on growth, herbage production, and herbage content. Conversely, water stress had a positive influence on the essential oil content of the plants. Based on the findings, it can be concluded that the application of 50 Mg ha<sup>-1</sup> fertilizer resulted in a significant increase in biomass production compared to the other treatments.

**Keywords:** Acrylamide, Growth, Yield, Graft-copolymerization, Irrigation regimes, Biochar

## INTRODUCTION

Population growth, water scarcity, and climate change are pressing concerns with a profound impact on the agricultural sector. Enhancing the efficiency of fertilizer and water application is crucial for achieving optimal plant growth, particularly in drought-affected regions [1,2]. An estimated range of 40–70% of nitrogen (N), 80–90% of phosphorus (P), and 50–70% of potassium (K) applied through conventional fertilizer methods are subject to environmental losses [3]. The primary causes of these losses are surface runoff, leaching, and vaporization, resulting in significant environmental pollution and financial implications [4]. The use of environmentally-friendly superabsorbent polymers for encapsulating fertilizer particles proves to be an effective approach to mitigating these losses [5,6]. By applying these polymers, nutrients can be gradually released, resulting in efficient absorption by plants and a reduction in environmental pollution [7-10].

Superabsorbent polymers are hydrophilic, three-dimensional cross-linked structures that enable them to demonstrate remarkable water and solution absorption capabilities. These exceptional properties are attributed to factors such as their extra ionic cross-linking, undulated porous structure, abundance of hydrophilic groups, and high flexibility of polymer chains [11]. Various mechanisms, including radical polymerization, condensation polymerization, graft copolymerization, photopolymerization, and ring-opening polymerization, have been employed for synthesizing polymers [12,13]. The graft reaction is a polymer synthesis technique that involves the attachment of one or more monomers to the backbone of the polymer. During the graft reaction, an active site

is generated at a specific location along the polymer chain, separate from its end. This active site is subsequently exposed to a monomer, leading to the process of copolymerization [14]. Recent research has shown a significant interest in alginate-based graft copolymers, especially regarding the grafting of monomers like acrylic acid, acrylamide, methyl methacrylate, N-vinylpyrrolidone, and methacrylic acid [15-17].

Recently, there has been a growing interest in the production of environmentally-friendly superabsorbent polymers (SAPs) as an effective approach to regulating nutrient release and promoting environmental safety [18,19]. The biodegradation process of biodegradable materials is primarily facilitated by microorganisms, while environmental degradation is predominantly attributed to the hydrolysis and oxidation processes that occur in the environment [20]. The macromolecules of SAPs have the capability to undergo degradation, either the breaking down into smaller molecular compounds or undergoing complete decomposition. Polysaccharide-based materials, including starch, chitosan, alginate, and cellulose, are essential components of natural-based superabsorbent hydrogel materials due to their distinct characteristics, such as non-toxicity, renewability, biodegradability, and biocompatibility [21]. Among the various polysaccharide-based materials, alginic acid extracted from brown algae, specifically from the phylum Phaeophyta, stands out as a versatile polysaccharide with remarkable properties that significantly enhance its value in the production of superabsorbent materials. Alginates refer to the salts and derivatives derived from alginic acid, and sodium alginate stands as the most commonly utilized compound among all its variants [22]. The graft copolymerization of vinyl monomers onto alginates is a highly effective approach for the synthesis of SAPs [7].

*Thymus daenensis* Celak., an herb of the mint family (Lamiaceae), is indigenous to Iran and thrives in diverse regions throughout the country. This subspecies of *Thymus daenensis* Celak. is specifically recognized for its small aromatic leaves. During the flowering season, it produces clusters of purple or pink flowers. Researchers have conducted investigations on extracts or essential oils obtained from this subspecies to explore their potential health benefits. These studies have focused on various aspects, including antimicrobial, antioxidant, and anti-inflammatory activities, among others [23,24].

Based on previous research on the gradual nutrient release and slow-release fertilizer properties of biochar [25], this study utilized biochar as a nutrient supplier in the production of SSRF. The process of converting organic material into a stable carbon form is referred to as biochar. Biochar consists of elements including C, H, S, O, N, and minerals found in the ash fraction. Biochar is primarily produced through pyrolysis under controlled conditions with a limited oxygen supply [26,27]. The fertilizer in this study was prepared using rapeseed meal biochar that had been produced at a temperature of 300 °C.

The objective of this study was to examine the impact of water stress and the application rate of a novel superabsorbent fertilizer on the growth, essential oil yield, and essential oil content of *Thymus daenensis* in drainage lysimeters filled with sandy loam soil in a semi-arid region. The distinctive feature of this study lies in the utilization of rapeseed meal biochar as a nutrient source for producing SSRF, along with the incorporation of the grafting reaction of acrylic acid and acrylamide onto the alginate backbone. This study aims to explore the potential benefits and synergistic effects of the novel fertilizer in mitigating the impact of water deficit on herbage biomass and oil yield in *Thymus daenensis*. The integration of a slow-release fertilizer with water management strategies represents a novel approach that can contribute to sustainable cultivation practices and enhance the productivity of *Thymus daenensis* in water-limited environments.

## **MATERIAL AND METHODS**

### **Materials**

Sodium alginate (NaAlg), methylenebisacrylamide, ammonium persulfate, calcium chloride monohydrate ( $\text{CaCl}_2 \cdot \text{H}_2\text{O}$ ) and acrylic acid, and acrylamide were employed in the graft copolymerization process as the polymer backbone, crosslinking agent, initiator, precipitating agent, and monomers, respectively. Acrylamide, acrylic acid, and ammonium persulfate were sourced from Merck Corporation (Germany), whereas calcium chloride monohydrate and sodium alginate were obtained from R&M (UK).

### **Preparation of Biochar**

Rapeseed meal was used as the feedstock for the production of biochar. The rapeseed powder was initially dried under ambient air conditions, followed by grinding and sieving to acquire particle sizes smaller than 2 mm. An

electrical furnace housed within a specially designed cubic iron box was used to produce biochar. The box's door included an inlet for introducing nitrogen gas, as well as an outlet for the release of generated gases. The feedstock underwent pyrolysis by being exposed to a temperature of 300 °C with a heating rate of 5 °C per minute. It was maintained at this temperature for a period of 2 hours. The prepared biochar was analyzed to determine the content of nitrogen (N), carbon (C), hydrogen (H), sulfur (S), and oxygen (O). The analysis was revealed that the biochar contained 14.8% N, 60.15% C, 5.1% H, 0.5% S, and 19.45% O by weight (w%). Furthermore, the pH value of the biochar was determined to be 8.67. The electrical conductivity (EC) of the biochar was measured at 2 dS/m, and the specific surface area was determined to be 70 m<sup>2</sup>/g.

### Characterization Measurement

The CHNS elements of the rapeseed meal biochar were analyzed using a Vario EL III instrument from Germany. The O element content was determined through the difference calculation of the CHNS measurements. A Kjeldahl method was employed to determine the N content of the soil, while the inductively coupled plasma optical emission spectrometry (ICP-OES) technique, using the PerkinElmer Optima 7300DV instrument, was used to measure the P and K contents. A Belsorp mini II instrument from Japan was utilized to measure the BET surface area. This was done by employing N<sub>2</sub> adsorption-desorption isotherms at a temperature of 196 °C and a relative pressure of 0.98. The surface morphology of the fertilizer was examined using Scanning Electron Microscopy (SEM) with a Philips XI30 instrument from the Netherlands.

### Preparation of Superabsorbent Polymer

To form a gelatinized sodium alginate paste, 8 g of sodium alginate were dispersed in 200 mL of deionized water. The resulting system was then subjected to heating at 80 °C with simultaneous mechanical stirring at 1000 rpm for a duration of 20 min. After cooling, the gelatinized sodium alginate paste was combined with 20 g of acrylic acid and acrylamide in a 50:50 concentration ratio. Additionally, 0.2 g of methylenebisacrylamide was added to the mixture. Then, 1 g of ammonium persulfate was introduced as an initiator, and the mixture was subjected to stirring at 1000 rpm for a duration of 120 min. The biochar particles were blended and stirred with the resulting gel to achieve uniformity. The gel was subsequently precipitated by being dropped from a separating funnel into a beaker containing a 2 mol L<sup>-1</sup> calcium chloride monohydrate solution. It was then placed in the solution for 1 hour. Afterward, the beads were removed from the liquid mixture, washed with deionized water, and dried overnight at 60 °C. Following grafting, the graft copolymer is typically purified by completely extracting the monomer from the mixture using acetone.

### Swelling Capacity

The swelling capacity of SSRF was assessed using the tea bag method as described by Huang *et al.* [28]. To achieve equilibrium swelling, the SSRF sample was enclosed in a tea bag and immersed in an excess amount of water for a duration of 1 h. Any excess solution was then removed by suspending the bag until no liquid droplets were observed. The swelling capacity ( $S_e$ ) was determined using Equation 1:

$$S_e = \frac{W_2 - W_1}{W_1} \quad (1)$$

Where  $W_1$  represents the weight of the polymer before swelling, and  $W_2$  represents the weight of the polymer after swelling.

### The rate of SSRF Release in Soil

In order to ascertain the rate of SSRF release in soil, an experiment was conducted as follows: a blend of 1 g of SSRF and 200 grams of dry soil was thoroughly mixed and transferred to a covered 200 mL beaker. Subsequently, the beaker was incubated at room temperature for varying time durations. The measured values of phosphorus (P), potassium (K), magnesium (Mg), calcium (Ca), and nitrate nitrogen (N-NO<sub>3</sub><sup>-</sup>) in the studied soils were 18.5 mg/L, 306 mg/L, 90 mg/L, 110 mg/L, and 10 mg/L, respectively. Additionally, the organic matter (OM) content, electrical conductivity (EC), and pH were determined to be 0.25 g/Kg, 0.95 dS/m, and 7.5, respectively. During the experiment, the soil was consistently retained at a water-holding capacity of 20 wt% by monitoring its weight and adding distilled water as needed. At intervals of 1, 3, 5, 10, 15, 20, 25, and 30 days, the remaining SSRF in

the beakers was extracted, washed, and then air-dried overnight. This procedure facilitated the estimation of N, P, and K contents.

### Field Study

The experiment was performed for one year at the experimental farm of Isfahan University of Technology, utilizing 27 drainage lysimeters. Each lysimeter had a diameter of 0.5 m and a depth of 0.9 m. These lysimeters were filled with sandy loam soil and equipped with an outlet at the bottom to facilitate the collection of leachate at atmospheric pressure. As shown in Figure 1, the lysimeter experiment employed three irrigation treatments with three replications: intensive stress (50% water requirement), moderate stress (70% water requirement), and no water stress (100% water requirement). The lysimeters were irrigated using a hosepipe. The determination of reference evapotranspiration was accomplished through the utilization of the FAO-Penman-Monteith method, with the assistance of CROPWAT 8.0 software. The fertilizer application rates in the experiment were 10 and 50 ton/ha, while the control treatment involved the absence of fertilizer application to the soil. One week after reaching the full flowering stage, the plants were harvested by cutting them 5 cm above the soil surface. Following that, measurements of plant height and aerial fresh weight were taken during the harvest. To ascertain the dry weight, the aerial portion of the plants was dried in the absence of light at a temperature of 40°C until a consistent weight was attained. The measurement of plant height involved determining the distance from the soil surface to the apex of the tallest flowering stem. The essential oil was extracted from the dried leaves and flowers using hydro distillation in a Clevenger-type apparatus, following the guidelines outlined in the British Pharmacopoeia. The essential oil content was determined and expressed as a relative percentage, while the total essential oil yield was calculated by multiplying the dry matter by the oil content.

### Data Analysis

The data were analyzed using the IBM SPSS Statistics 22 software package. The values for each treatment were calculated as the mean of three replicates  $\pm$  standard deviation (S.D.). Statistical comparisons between means were performed using the LSD test with a significance level of  $p < 0.05$ .

**Fig. 1** Drainage lysimeters used in the experimental setup to investigate the impact of fertilizer and water deficit on herbage biomass and oil production.



## RESULTS

### Characterization



Figure 2 presents the SEM images of the SSR. Figure 2a illustrates the coarse and undulant texture of the SSRF's surface, leading to an augmented specific surface area. The SEM analysis also reveals the presence of multiple small, uniform, and interconnected pores on the surface of SSRF. These pores served as sites of water permeation, facilitating the easy diffusion of water into the polymeric network. This resulted in the formation of a swollen hydrogel due to the absorption of water by the SSRF [29]. The observed surface morphology provided evidence for the occurrence of graft polymerization. The presence of large pores in the SSRF contributes to its high water retention and swelling rate. Figure 2b depicts the inner structure of the product, revealing a broad network and porous configuration. Similar findings have been reported by Zhang *et al.* [29].

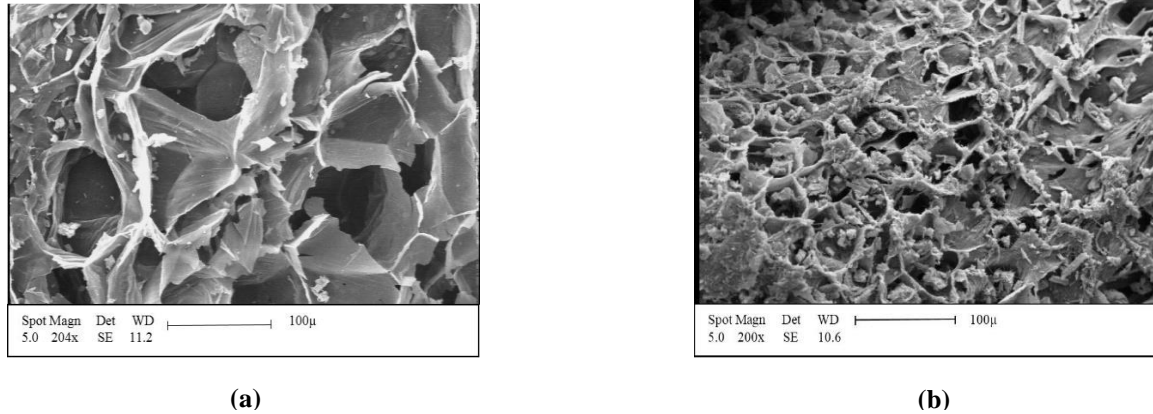


**Fig. 2** SEM images of (a) the outer surface and (b) the inner surface of prepared superabsorbent slow-release fertilizer.

The grafted polymer demonstrated a nitrogen percentage of 21%, which is consistent the findings reported by Wu *et al.* [3], who obtained a nitrogen content of 15.7%. The produced fertilizer exhibited a swelling capacity of 40% when evaluated using the tea bag method. The high water absorbency of SSRF can be attributed to several factors, including the presence of hydrophilic groups, the crosslinking density of the polymer, the behavior of the polymer network, and the elasticity of the polymer networks [30]. These factors collectively contribute to SSRF's to efficiently absorb water.

The slow-release property is considered one of the key characteristics of SSRF. Figure 3 illustrates the slow-release behavior of N, P, and K from the fertilizer when applied to soil. According to the Figure, the release rate of N is comparatively higher compared to that of P and K. This can be attributed to the high solubility of urea, which enabled its rapid dissolution and subsequent release into the soil. Over a period of 30 days, the release rates of N, P, and K were determined to be 83%, 58%, and 46%, respectively.

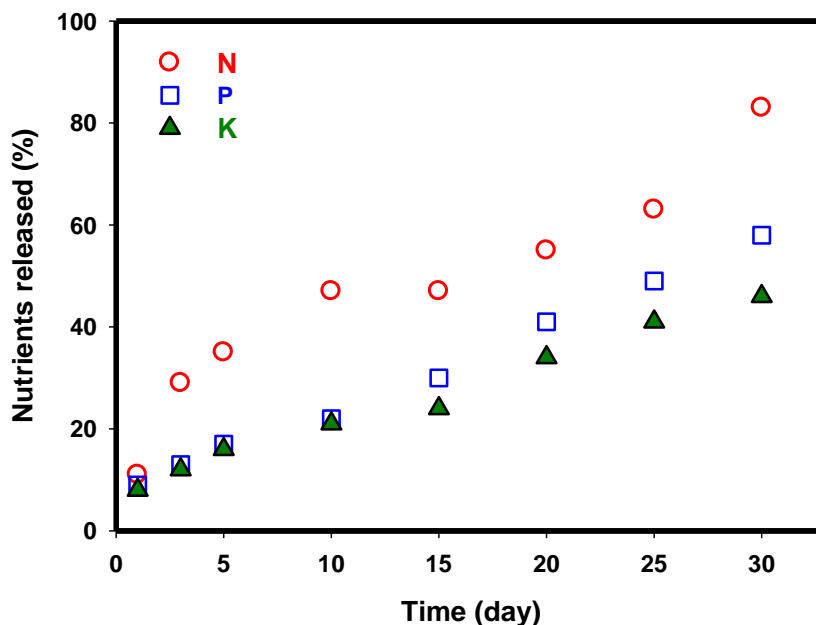


**Fig. 3** The release behavior of N, P, and K from the fertilizer in the soil.

The proposed mechanism for the release of NPK from the fertilizer into the soil is described as follows: (1) dissolution: when the fertilizer is exposed to soil moisture, it undergoes dissolution, resulting in the release of soluble compounds that contain N, P, and K; (2) ion exchange; ion exchange occurs when the NPK compounds undergo dissolution and interact with soil. This process facilitates the release of nutrients from the fertilizer and their subsequent binding to the cation exchange sites in the soil; (3) diffusion: diffusion occurs as the released NPK nutrients move through the soil matrix, diffusing from regions of higher concentration near the fertilizer to regions of lower concentration in the surrounding soil; (4) microbial processes: microbial processes also play a crucial role in the nutrient-release process. Soil microorganisms, such as bacteria and fungi, contribute to the breakdown of organic matter within the soil; (5) plant uptake: during the process of nutrient diffusion in the soil, plant roots actively and passively absorb the nutrients through various uptake mechanisms.

## Field Study Results

When investigating water stress, three crucial traits that are widely regarded as significant include plant growth, survival, and plant water status [31,32]. Water stress is typically characterized by lower water potential, reduced water content, diminished plant growth, and, ultimately, wilting [33]. In the present study, growth indicators such as plant height, dry weight, and fresh weight were recorded. Additionally, the study investigated the impact of water stress and SSRF application rate on the essential oil content and yield of the plant.

## Effect of Water Deficit and SSRF on Plant Morphology and Herbage Production

The results revealed significant interaction effects between SSRF and water treatment on almost all the growth parameters, including the essential oil content and yield of *T. daenensis*, as presented in Table 1. The study found that the effects of water stress treatment, SSRF rate, and the interaction between water stress treatment and SSRF rate on plant height, fresh weight, dry weight, and essential oil percentage of *Thymus daenensis* were significant. These findings are presented in Table Under normal irrigation conditions, it was observed that the highest herbage dry and fresh weights of *T. daenensis* were achieved when the highest rate of fertilizer (50 ton/ha) was applied.

**Table 1** Analysis of variance (mean of squares) for the effect of SSRF and water stress treatment on the measured properties of *T. daenensis*.

Source of variation	df <sup>1</sup>	Plant height (cm)	Fresh weight (kg/ha)	dry weight (kg/ha)	Essential oil content	Essential oil yield
Model	8	22.954 **	3740325.863 **	513076.25 **	0.478 **	110.07 **
Water stress treatment	2	76.747 **	3309.63 **	1974133 **	1.807 **	388.96 **
Fertilizer rate	2	14.384 **	115.858 **	69107.444 **	0.099 **	99.959 **
Water stress treatment × Fertilizer rate	4	0.343 **	33040.305 **	4532.278 **	0.003 **	0.68 ns
Error	18	0.117 **	4348.5	596.481	0	0.327

<sup>1</sup> degree of freedom; \*\* indicates significant effect at  $p < 0.01$ .

The study found that water stress had a significant effect on plant height, as well as dry and fresh weights. Furthermore, the impact of water stress on these parameters became more pronounced with an increase in the severity of water stress. These findings are illustrated in Table 2. The study observed that plants exposed to severe water deficit without the application of superabsorbent fertilizer had thinner stems and smaller leaves compared to plants not experiencing water stress. The observed phenomenon aligns with expectations, as it is well-known that plants tend to produce less biomass when subjected to water stress.

**Table 2** Means' comparisons of plant height, dry and fresh weights of areal parts of plant as affected by water stress levels.

Water stress level	Plant height (cm)	Fresh weight (kg/ha)	Dry weight (kg/ha)
Full irrigation	23.611 a	4275.3 a	1583.444 a
70% water requirement	23.222 b	2994.6 b	1109.111 b
50% water requirement	18.37 c	1746.3 c	646.778 c

Values in columns with different superscripts (a–c) indicate significant differences at  $p < 0.05$ , based on the means of three replicates.

Means' comparisons of the results showed a significant ( $p < 0.05$ ) decrease in plant height, as well as dry and fresh weights, as the SSRF rate decreased. As a result, the plants exhibited the highest plant height, dry weight, and fresh weight for their aerial parts when the highest rate of fertilizer (50 ton/ha) was applied. The inclusion of element contents in the fertilizer led to an increase in nutrient absorption, and this effect was further enhanced with higher fertilizer rates. These characteristics exhibited a significant increase ( $p < 0.05$ ), as evidenced by the data presented in Table 3.

**Table 3** Effects of fertilizer rate on plant height, dry and fresh weights of areal parts of plant.

Fertilizer rate (Mg/ha)	Plant height (cm)	Fresh weight (kg/ha)	Dry weight (kg/ha)
0	20.422 a	2753.1 a	1019.667 a
10	21.837 b	3040.8 b	1126.222 b
50	22.944 c	3222.3 c	1193.444 c

Values in columns with different superscripts (a–c) indicate significant differences at  $p < 0.05$ , based on the means of three replicates.

The decrease in plant height, as well as dry and fresh weights, observed under water stress can be attributed to a decline in cell enlargement and an increase in leaf senescence. These effects occur due to a decrease in turgor pressure within the plant cells [34]. The decrease in plant height, as well as dry and fresh weights, under water stress can be attributed to either a preferential allocation of biomass production to the roots or a reduction in chlorophyll content. These factors ultimately lead to a decrease in photosynthesis efficiency [35]. The decrease in both fresh and dry weights of the plant can also be attributed to various factors associated with water stress. These factors include decreased plant growth, impaired photosynthesis, and alterations in canopy structure. These combined effects collectively contribute to the observed decrease in biomass accumulation under water stress conditions.

Furthermore, the limited availability of moisture in the root zone leads to a decrease in root biomass proliferation. In turn, this leads to a decrease in the absorption of nutrients and water, ultimately resulting in reduced biomass production [36]. The analysis of variance demonstrated that the rate of fertilizer application had a significant impact on both the yield of dry and fresh weights of the plants, as indicated in Table 3. The decrease in plant height, as well as dry and fresh weights observed in this study, aligns with the findings reported by Letchamo and Gosselin [37] for *T. vulgaris*, Bettaieb *et al.* [38] for *Salvia officinalis*, and Laribi *et al.* [39] for *Carum carvi*. A study conducted by Bahreinejad *et al.* [23] evaluated the effects of different levels of soil water depletion (20%, 50%, and 80%) on the growth of *Thymus daenensis*. The results indicated that water stress had a negative impact on plant growth, herbage production, as well as chlorophyll and carotenoid content. However, it led to an increase in the essential oil content of the plant. In addition, it was found that irrigation water use efficiency, based on essential oil yield, increased under water stress conditions. Similar findings were reported by Emami Bistgani *et al.* [40], who observed a significant decrease in the dry matter yield of *Thymus daenensis* with increasing severity of drought stress. In a separate study conducted by Yi *et al.* [41], similar findings were reported regarding the effect of biochar on N uptake. The application of biochar was found to significantly enhance the uptake of N by plants. Our findings demonstrate that the superabsorbent fertilizer produced with biochar exhibits similar characteristics to biochar, such as slow-release of nutrients. Additionally, it exhibits the water retention capacity commonly found in conventional polymer hydrogels. In a comparable study conducted by Satriani *et al.* [42], it was demonstrated that applying superabsorbent hydrogel to plants experiencing drought stress effectively maintained high soil water potential and water content.

### Effect of Water Deficit and Super Absorbent Fertilizer on Essential oil Content and Yield

The study findings indicated that under water stress conditions, there was an observed increase in the essential oil content of the plants. However, there was also a simultaneous decrease in the essential oil yield, as reported in Table 4. A significant difference ( $p \leq 0.01$ ) was observed between the different irrigation treatments in terms of both essential oil yield and oil content. The full irrigation treatment yielded the highest amount of oil, while the severe drought stress treatment (50% water requirement) showed the highest oil content. The decrease in essential oil yield can be attributed to the decrease in herbage yield, as shown in Table 2. This suggests a positive correlation between essential oil yield, soil water content, and herbage yield. Higher soil water content and greater

herbage yield have a positive impact on the production of essential oil. In fact, Emami Bistgani *et al.* [39] have reported that water stress can even result in an increase in essential oil accumulation. This is believed to happen due to a higher density of oil glands, which is a consequence of the reduction in leaf area caused by water stress. In addition, the elevation in essential oil concentration during water stress may be attributed to the plants' response to producing higher concentrations of terpene. This response is thought to occur because, during water stress, plants allocate less carbon to growth and instead prioritize defense mechanisms. This suggests a trade-off between growth and defense in the context of water stress.

**Table 4** Effect of water stress levels on essential oil content and yield.

Water stress level	Essential oil yield (kg/ha)	Essential oil content (%)
Full irrigation	28 a	1.766 a
70% water requirement	27.139 b	2.441 b
50% water requirement	16.966 c	2.613 c

Values in columns with different superscripts (a–c) indicate significant differences at  $p < 0.05$ , based on the means of three replicates.

As indicated in Table 5, an increase in the rate of fertilizer application leads to a simultaneous increase in both essential oil yield and essential oil content. Fertilizer application stimulates plant growth and enhances biomass production, resulting in a larger plant biomass. This increased biomass provides a larger capacity for essential oil synthesis and storage, ultimately leading to higher essential oil yield and content. Moreover, Fertilizers play a crucial role in supplying essential nutrients required for plant growth and development. By increasing the rate of fertilizer application, the availability of key nutrients such as N, P, and K is enhanced. These nutrients play a crucial role in various metabolic pathways, including the biosynthesis of essential oil compounds. Consequently, the increased availability of nutrients promotes the synthesis and accumulation of essential oils, resulting in higher essential oil yield and content.

**Table 5** Effect of fertilizer rate on essential oil content and yield.

Fertilizer rate (ton/ha)	Essential oil yield (kg/ha)	Essential oil content (%)
0	20.598 a	2.15 a
10	24.254 b	2.28 b
50	27.253 c	2.4 c

Values in columns with different superscripts (a–c) indicate significant differences at  $p < 0.05$ , based on the means of three replicates.

## CONCLUSION

An SSRF was synthesized using a graft copolymerization technique. In this process, sodium alginate, methylenebisacrylamide, ammonium persulfate, calcium chloride monohydrate, acrylic acid, and acrylamide were employed as the polymer backbone, crosslinking agent, initiator, precipitating agent, and monomers, respectively. Overall, SSRF's slow-release properties offer several advantages, including controlled nutrient release, prolonged nutrient availability, enhanced water-retention capacity and nutrient absorption. These features make SSRF a valuable choice for promoting efficient and responsible fertilization practices. Additionally, water stress was found to cause a decline in the growth and plant biomass of *Thymus daenensis* aerial parts. The interaction effects of SSRF and water stress treatment were found to be significant across almost all growth parameters, as well as the essential oil content and yield of *Thymus daenensis*. The most noteworthy discovery of the study is that significant water savings can be achieved by reducing irrigation water and utilizing superabsorbent polymers. These polymers are highly suitable for maintaining both herbage biomass and oil production. However, there are several limitations that should be considered: (a) limited generalizability to other plant species/varieties, as responses to the novel fertilizer and water deficit may vary; (b) variation in environmental conditions across locations/seasons may impact results and generalizability; (c) interactions with other factors (soil composition, nutrients, pests) can confound outcomes; (d) narrow focus on biomass and oil production overlooks other important parameters; (e) study duration may not capture long-term effects or full growth cycle of *Thymus daenensis*; (f) practical application and scalability challenges, including cost, availability,



and ease of application, which may impact the widespread adoption of the novel fertilizer in real-world agricultural settings

## Funding

This research received no external funding.

## Data Availability Statement

Data are available in the paper.

## Conflicts of Interest

The authors declare no conflict of interest.

## REFERENCES

1. Adam D. How Far Will Global Population Rise. *Nature*. 2021;597:462–465.
2. United Nations, Department of Economic and Social Affairs, Population Division. World Population Prospects 2019: Highlights (ST/ESA/SER.A/423). 2019. Available online: [https://population.un.org/wpp/publications/files/wpp2019\\_highlights.pdf](https://population.un.org/wpp/publications/files/wpp2019_highlights.pdf) (accessed on 1 July 2022).
3. Wu L., Liu M. Preparation and properties of chitosan-coated NPK compound fertilizer with controlled-release and water-retention. *Carbohydr. Polym.* 2008;72:240–247.
4. Kriech A.J., Osborn L.V. Review of the impact of stormwater and leaching from pavements on the environment. *J. Environ. Manage.* 2022;319:115687.
5. Kontárová S., Přikryl R., Škarpa P., Křiška T., Antošovský J., Gregušková Z., Figalla S., Jašek V., Sedlmajer M., Menčík P., et al. Slow-release nitrogen fertilizers with biodegradable poly(3-hydroxybutyrate) coating: their effect on the growth of maize and the dynamics of N release in soil. *Polymers*. 2022;14:4323. <https://doi.org/10.3390/polym14204323>
6. Kareem S.A., Dere I., Gungula D.T., Andrew F.P., Saddiq A.M., Adebayo E.F., Tame V.T., Kefas H.M., Joseph J., Patrick D.O. Synthesis and characterization of slow-release fertilizer hydrogel based on hydroxy propyl methyl cellulose, polyvinyl alcohol, glycerol and blended paper. *Gels*. 2021;7:262. <https://doi.org/10.3390/gels7040262>
7. Baki M., Abedi-Koupai J. Preparation and characterization of a superabsorbent slow-release fertilizer with sodium alginate and biochar. *J. Appl. Polym. Sci.* 2018;135:45966.
8. Tian C., Zhou X., Ding Z., Liu Q., Xie G., Peng J., Eissa M.A. Controlled-release N fertilizer to mitigate ammonia volatilization from double-cropping rice. *Nutr. Cycl. Agroecosyst.* 2021;119:123–137.
9. Jia C., Lu P., Zhang M. Preparation and characterization of environmentally friendly controlled release fertilizers coated by leftovers-based polymer. *Processes*. 2020;8:417. <https://doi.org/10.3390/pr8040417>
10. Abedi-Koupai J., Eslamian S.S., Asad Kazemi, J. Enhancing the available water content in unsaturated soil zone using hydrogel, to improve plant growth indices. *Ecohydrol. Hydrobiol.* 2008;8:3–11.
11. Rather R.A., Bhat M.A., Shalla A.H. An insight into synthetic and physiological aspects of superabsorbent hydrogels based on carbohydrate type polymers for various applications: A review. *Carbohydr. Polym. Technol. Appl.* 2022;3:100202.
12. Das A., Ringu T., Ghosh S., et al. A comprehensive review on recent advances in preparation, physicochemical characterization, and bioengineering applications of biopolymers. *Polym. Bull.* 2023;80:7247–7312. <https://doi.org/10.1007/s00289-022-04443-4>
13. Namsheer K., Rout C.S. Conducting polymers: a comprehensive review on recent advances in synthesis, properties and applications. *RSC Adv.* 2021;11:5659–5697.
14. Sand A., Vyas A., Gupta A. Graft copolymer based on (sodium alginate-g-acrylamide): characterization and study of water swelling capacity, metal ion sorption, flocculation and resistance to biodegradability. *Int. J. Biol. Macromol.* 2016;90:37–43.
15. Safakas K., Saravanou S.-F., Iatridi Z., Tsitsilianis C. Thermo-responsive injectable hydrogels formed by self-assembly of alginate-based heterograft copolymers. *Gels*. 2023;9:236. <https://doi.org/10.3390/gels9030236>
16. Saravanou S.F., Ioannidis K., Dimopoulos A., Paxinou A., Kounelaki F., Varsami S.M., Tsitsilianis C., Papantoniou I., Pasparakis G. Dually crosslinked injectable alginate-based graft copolymer thermoresponsive hydrogels as 3D printing bioinks for cell spheroid growth and release. *Carbohydr. Polym.* 2023;312:120790.
17. Darwesh H., Mohamed, R.R., Soliman, S.M.A. Synthesis of novel antibacterial grafted sodium alginate copolymer-based adsorbent for wastewater treatment. *Polym. Bull.* 2023. In press. <https://doi.org/10.1007/s00289-023-04754-0>
18. Li T., Lü S., Zhang S., Gao C., Liu M. Lignin-based multifunctional fertilizer for immobilization of Pb (II) in contaminated soil. *J. Taiwan Inst. Chem. Eng.* 2018;91:643–652.

19. Li H., Yang L., Cao J., Nie C., Liu H., Tian J., Chen W., Geng P., Xie, G. Water-preserving and salt-resistant slow-release fertilizers of polyacrylic acid-potassium humate coated ammonium dihydrogen phosphate. *Polymers*. 2021;13:2844. <https://doi.org/10.3390/polym13172844>
20. Azeem B., Shaaria K., Mana Z. Review on materials & methods to produce controlled release coated urea fertilizer. *Procedia. Eng.* 2016;148:282–289.
21. Chen C., Xi Y., Weng Y. Recent advances in cellulose-based hydrogels for tissue engineering applications. *Polymers*. 2022;14:3335. <https://doi.org/10.3390/polym14163335>
22. Abka-khajouei R., Tounsi L., Shahabi N., Patel A.K., Abdelkafi, S., Michaud P. Structures, properties and applications of alginates. *Mar. Drugs*. 2022;20:364. <https://doi.org/10.3390/md20060364>
23. Bahreininejad B., Razmjoo, J., Mirzab M. Influence of water stress on morpho-physiological and phytochemical traits in *Thymus daenensis*. *Int. J. Plant. Product*. 2013;7(1):151–166.
24. Norouzi Y., Ghobadi M., Saeidi M., Dogan H. Effect of nitrogen and cytokinin on quantitative and qualitative yield of Thyme (*Thymus vulgaris* L.). *Agrotechniques in Industrial Crops*. 2021;1(1):52-60. doi: 10.22126/etic.2021.6481.1012
25. Wang C., Luo D., Zhang X., Huang R., Cao Y., Liu G., Zhang Y., Wang H. Biochar-based slow-release of fertilizers for sustainable agriculture: A mini review. *Environ. Sci. Ecotechnology*. 2022;10:100167.
26. Amiri M.J., Bahrami M., Beigzadeh B., Gil A. A response surface methodology for optimization of 2, 4-dichlorophenoxyacetic acid removal from synthetic and drainage water: A comparative study. *Environ. Sci. Pollut. Res.* 2018;25:34277–34293.
27. Amiri M.J., Roohi R., Arshadi M., Abbaspourrad A. 2,4-D adsorption from agricultural subsurface drainage by canola stalk-derived activated carbon: Insight into the adsorption kinetics models under batch and column conditions. *Environ. Sci. Pollut. Res.* 2020;27:16983–16997.
28. Huang M., Shen X., Sheng X., Fang Y. Study of graft copolymerization of N-maleamic acid-chitosan and butyl acrylate by  $\gamma$ -ray irradiation. *Int. J. Biol. Macromol.* 2005;36:98.
29. Zhang M., Zhang S., Chen Z., Wang M., Cao J., Wang R. Preparation and Characterization of Superabsorbent Polymers Based on Sawdust. *Polymers*. 2019;11:1891. <https://doi.org/10.3390/polym11111891>
30. Qi Z., Hu X. Water absorbency of super absorbent polymer based on flexible polymeric network. *Eur. Polym. J.* 2022;166:111045.
31. Osakabe Y., Osakabe K., Shinozaki K., Tran L-S.P. Response of plants to water stress. *Front. Plant Sci.* 2014;5:86. <https://doi.org/10.3389/fpls.2014.00086>
32. Abedi-koupai J., Mollaei R., Eslamian S.S. The effect of pumice on reduction of cadmium uptake by spinach irrigated with wastewater. *Ecohydrol. Hydrobiol.* 2015;15(4):208-214.
33. Zhao W., Liu L., Shen Q., Yang J., Han X., Tian F., Wu J. Effects of water stress on photosynthesis, yield, and water use efficiency in winter wheat. *Water*. 2020;12:2127. <https://doi.org/10.3390/w12082127>
34. Shao H.B., Chu L.Y., Jaleel C.A., Zhao C-X. Water-deficit stress-induced anatomical changes in higher plants. *C. R. Biologies*. 2008;331:215–225.
35. Loudari A., Mayane A., Zeroual Y., Colinet G., Oukarroum, A. Photosynthetic performance and nutrient uptake under salt stress: differential responses of wheat plants to contrasting phosphorus forms and rates. *Front. Plant Sci.* 2022;13:1038672. <https://doi.org/10.3389/fpls.2022.1038672>
36. Liang S., Li L., An P., Chen S., Shao L., Zhang, X. Spatial soil water and nutrient distribution affecting the water productivity of winter wheat. *Agric. Water Manag.* 2021;256:107114. <https://doi.org/10.1016/j.agwat.2021.107114>
37. Letchamo W., Gasselín A., Transpiration, essential oil glands, epicuticular wax and morphology of *Thymus vulgaris* are influenced by light intensity and water supply. *J. Hortic. Sci.* 1996;71:123–134.
38. Bettaieb I., Zakhama N., Aidi Wannes W., Kchouk M.E., Marzouk, B. Water deficit effects on *Salvia officinalis* fatty acids and essential oils composition. *Sci. Hort.* 2009;120:271–275.
39. Laribi B., Bettaieb I., Kouki K., Sahli A., Mougou A., Marzouk B. Water deficit effects on caraway (*Carum carvi* L.) growth, essential oil and fatty acid composition. *Ind. Crops. Prod.* 2009;30(3):372–379.
40. Emami Bistgani Z., Siadat S.A., Bakhshandeh A., Pirbalouti A.G., Hashemi M. Interactive effects of drought stress and chitosan application on physiological characteristics and essential oil yield of *Thymus daenensis* Celak. *Crop J.* 2017;5:407-415.
41. Yi Z., Jeyakumar P., Yin C., Sun H. Effects of biochar in combination with varied N inputs on grain yield, N uptake,  $\text{NH}_3$  volatilization, and  $\text{N}_2\text{O}$  emission in paddy soil. *Front. Microbiol.* 2023;14:1174805. <https://doi.org/10.3389/fmicb.2023.1174805>
42. Satriani A., Catalano M., Scalcione E. The role of superabsorbent hydrogel in bean crop cultivation under deficit irrigation conditions: A case-study in Southern Italy. *Agric. Water. Manag.* 2018;195:114–119.